



Published in final edited form as:

Heart Rhythm. 2008 August ; 5(8): 1170–1177. doi:10.1016/j.hrthm.2008.04.009.

Intracellular calcium dynamics and acetylcholine-induced triggered activity in the pulmonary veins of dogs with pacing-induced heart failure

Chung-Chuan Chou, MD^{*}, Bich Lien Nguyen, MD[†], Alex Y. Tan, MD[‡], Po-Cheng Chang, MD^{*}, Hui-Ling Lee, MD[†], Fun-Chung Lin, MD^{*}, San-Jou Yeh, MD^{*}, Michael C. Fishbein, MD[¶], Shien-Fong Lin, PhD[§], Delon Wu, MD^{*}, Ming-Shien Wen, MD^{*}, and Peng-Sheng Chen, MD, FHR[§]

^{*} Second Section of Cardiology, Department of Medicine, Chang Gung Memorial Hospital and Chang Gung University College of Medicine, Taoyuan, Taiwan

[†] Department of Anesthesia, Chang Gung Memorial Hospital and Chang Gung University College of Medicine, Taoyuan, Taiwan

[‡] Division of Cardiology, Department of Medicine, Cedars-Sinai Medical Center, Los Angeles California

[¶] Division of Anatomical Pathology, Department of Pathology, UCLA, Los Angeles, California

[§] Krannert Institute of Cardiology and Division of Cardiology, Department of Medicine, Indiana University School of Medicine, Indianapolis, Indiana

Abstract

BACKGROUND—Heart failure increases autonomic nerve activities and changes intracellular calcium (Ca_i) dynamics.

OBJECTIVE—The purpose of this study was to investigate the hypothesis that abnormal Ca_i dynamics are responsible for triggered activity in the pulmonary veins (PVs) during acetylcholine infusion in a canine model of heart failure.

METHODS—Simultaneous optical mapping of and membrane Ca_i potential was performed in isolated Langendorff-perfused PV–left atrial (LA) preparations from nine dogs with ventricular pacing-induced heart failure. Mapping was performed at baseline, during acetylcholine ($1 \mu\text{mol/L}$) infusion ($N = 9$), and during thapsigargin and ryanodine infusion ($N = 6$).

RESULTS—Acetylcholine abbreviated the action potential. In four tissues, long pauses were followed by elevated diastolic Ca_i , late phase 3 early afterdepolarizations, and atrial fibrillation (AF). The incidence of PV focal discharges during AF was increased by acetylcholine from 2.4 ± 0.6 beats/s ($N = 4$) to 6.5 ± 2.2 beats/s ($N = 8$; $P = .003$). PV focal discharge and PV–LA microreentry coexisted in 6 of 9 preparations. The spatial distribution of dominant frequency demonstrated a focal source pattern, with the highest dominant frequency areas colocalized with PV focal discharge sites in 35 (95%) of 37 cholinergic AF episodes ($N = 8$). Thapsigargin and ryanodine infusion eliminated focal discharges in 6 of 6 preparations and suppressed the inducibility of AF in 4 of 6 preparations. PVs

Address correspondence: Dr. Peng-Sheng Chen, Krannert Institute of Cardiology, Department of Medicine, Indiana University School of Medicine, 1801 N. Senate Avenue, E475, Indianapolis, Indiana 46202. chenpp@iupui.edu.
This manuscript was processed by a guest editor.

Supplementary data

Supplementary data associated with this article can be found, in the online version, at 10.1016/j.hrthm.2008.04.009.

with focal discharge have higher densities of parasympathetic nerves than do PVs without focal discharges ($P = .01$), and periodic acid–Schiff (PAS)-positive cells were present at the focal discharge sites.

CONCLUSION— Ca_i dynamics are important in promoting triggered activity during acetylcholine infusion in PVs from pacing-induced heart failure. PV focal discharge sites have PAS-positive cells and high densities of parasympathetic nerves.

Keywords

Acetylcholine; Atrium; Calcium; Fibrillation; Heart failure; Mapping

Introduction

Direct autonomic nerve recordings in a canine heart failure model show that not only sympathetic but also vagal nerves discharges are increased in heart failure, and simultaneous sympathovagal discharges are common triggers of atrial arrhythmias.¹ Vagal activation is thought to promote atrial fibrillation (AF) by shortening the refractory period, which accelerates and stabilizes reentrant excitation.² However, acetylcholine infusion also may induce late phase 3 early afterdepolarizations and triggered activity in normal canine atria³ if acetylcholine-induced action potential duration (APD) shortening is coupled with increased intracellular calcium (Ca_i) transient. The large and persistent Ca_i transient that occurs in late diastole activates the Na^+/Ca^{2+} exchanger (NCX), leading to afterdepolarizations and triggered activity.⁴ Heart failure is associated with abnormal Ca_i handling and increased NCX activity.⁵ The purpose of this study was to perform high-density simultaneous membrane potential (V_m) and Ca_i mapping⁶ to determine if Ca_i dynamics are directly responsible for triggered activity in the pulmonary veins (PVs) during acetylcholine infusion in a canine model of pacing-induced heart failure. A second aim of the study was to perform immunohistochemical studies to test the hypothesis that autonomic innervation and specialized conducting cells are juxtaposed to the PV focal discharge sites.

Methods

The research protocol was approved by the Institutional Animal Care and Use Committees of Chang Gung Memorial Hospital. Nine mongrel dogs (weight 16–29 kg) were used in the study. Under isoflurane anesthesia, the chest was opened via right thoracotomy. A screw-in bipolar pacing lead was inserted into the right ventricle and connected to an Itriel III neurostimulator (Medtronic, Inc., Minneapolis, MN, USA) for chronic pacing at 240 bpm starting 2 days after implantation until heart failure was induced.

Optical mapping studies

Hearts were rapidly removed, and the left coronary arteries were immediately cannulated and perfused with cold cardioplegic solution (4°C). Ventricular tissue 1 cm below the AV groove was quickly removed. The PV–left atrial (LA) preparation was placed in a tissue bath perfused and superfused with oxygenated Tyrode's solution of the following composition (in mmol/L): NaCl 125, KCl 4.5, $MgCl_2$ 0.25, $NaHCO_3$ 24, NaH_2PO_4 1.8, $CaCl_2$ 1.8, glucose 5.5, and albumin 50 mg/L in deionized water at $36.5^\circ C \pm 0.5^\circ C$, equilibrated with 95% O_2 and 5% CO_2 to maintain pH of 7.4. The hearts were double stained with rhod-2 AM and RH 237 (Molecular Probes, CA, USA) and then illuminated with laser (Millennia, Spectra-Physics Inc, CA, USA) at a wavelength of 532 nm. The emitted fluorescence was filtered through a 585 ± 20 -nm bandpass filter for Ca_i recording and a 710-nm long-pass filter for V_m recording. The fluorescence then was acquired simultaneously with two charge-coupled device cameras (CA-D1-0128T, Dalsa Inc, Ontario, Canada) at 4 ms per frame. The digital images (128×128 pixels)

were gathered from the epicardium of the left PVs and adjacent LA over a $25 \times 25\text{-mm}^2$ area. The mapped fields of the two cameras were spatially matched using epicardial registration points. Motion artifacts were suppressed by $5 \mu\text{mol/L}$ cytochalasin D (Sigma Aldrich Inc, MO). The fluorescence level of each pixel was compared with average fluorescence (\bar{F}) and color coded with shades of red for $>\bar{F}$ or blue for $<\bar{F}$ and animated to show the patterns of propagation.

Atrial arrhythmias were induced by S_1S_2 pacing and burst atrial pacing protocols. Three to five episodes of AF were mapped consecutively within the first 2 minutes after induction. Spontaneous atrial electrical activities were mapped to determine the sources of focal discharges and the patterns of initiation, if any. After the baseline studies, acetylcholine $1 \mu\text{mol/L}$ was infused for 15 minutes and the same pacing protocols repeated. Then ryanodine $2 \mu\text{mol/L}$ and thapsigargin $1 \mu\text{mol/L}$ were infused for 15 minutes and the same pacing protocols repeated in the presence of acetylcholine in 6 of 9 preparations.

Immunohistochemical studies

Hearts were fixed in Carnoy's solution immediately after mapping studies. Serial $5\text{-}\mu\text{m}$ -thick sections were immuno-stained with anti-choline acetyltransferase (ChAT; AB144P $200 \mu\text{L}$, Chemicon, Millipore, Inc, MA) and anti-tyrosine hydroxylase (TH; BYA90291, Accurate Chemical and Scientific Corporation, NY) antibodies to label cholinergic and adrenergic nerves, respectively. Periodic acid-Schiff (PAS) method (Accustain Schiff's reagent, Sigma-Aldrich, Inc, MO, USA) was used to stain for cellular glycogen content.⁶

Data analysis

Focal discharge was defined as an activation pattern with wavefronts spreading outward in all directions. The overall incidence of focal discharge was calculated by the average of the total number of focal discharges in 4 seconds. APD_{80} was the interval between phase 0 and the time of 80% repolarization, measured at a pacing cycle length of 500 ms. Monoexponential fit was used to compute the time constant of the decline of Ca_i transient (τ) at a pacing cycle length of 1,000 ms. APD_{80} and τ values in four nonpaced PV-LA preparations from normal dogs used in a previously published study⁶ were measured for control. Fast Fourier transform was used to determine the frequency at each pixel during 4 seconds of AF. The dominant frequency maps were constructed by plotting the dominant frequency of activation at different mapped regions.

Nerve density was quantified by a single blinded investigator using computer-assisted histomorphometry⁷ on pictures taken with a $40\times$ objective lens. Small nerve twigs, nerve trunks, and ganglion cells were included in the density calculation. Continuous variables are expressed as mean \pm SD. Paired or unpaired Student's tests were used to compare the means between two groups. $P \leq .05$ was considered significant.

Results

Left ventricular ejection fraction decreased from $54\% \pm 16\%$ to $26\% \pm 8\%$ ($N = 9$; $P < .001$) after 42 ± 7 days of rapid pacing. Compared with nonpaced normal dogs (137 ± 15 ms, $N = 4$), APD_{80} was longer in heart failure dogs (214 ± 16 ms, $N = 9$; $P < .001$). Mean τ of Ca_i decline was larger in the heart failure group (26.0 ± 4.5 ms, $N = 9$) than in the nonpaced control group (18.6 ± 0.4 ms, $N = 4$). Acetylcholine significantly shortened APD_{80} (80 ± 42 ms, $N = 9$; $P < .001$) but increased mean τ of Ca_i decline (33.5 ± 6.2 ms, $N = 9$; $P = .007$) in heart failure dogs.

Spontaneous focal discharge from PVs

Two episodes of spontaneous PV focal discharge were captured in two preparations at baseline and four episodes in four preparations during acetylcholine infusion. Figure 1 shows an example of PV focal discharge without acetylcholine infusion. The number below each map

is the time in milliseconds, with onset of data acquisition as time zero. Panel A shows Ca_i (yellow) and V_m (white) tracings recorded at the PV focal discharge site (asterisk, B). The underlying rhythm (beats 1, 2, and 3) was sinus rhythm. The wavefronts came from the right border of the mapped field, as shown by a representative V_m isochronal map (beat 3) in panel C. Three consecutive focal discharges (beats 4, 5, and 6) originated from the proximal left superior PV (LSPV). Panel D is a representative V_m isochronal map (beat 4) of these beats, showing the earliest activation site (black arrow) at the proximal LSPV. Panel E shows the Ca_i frame shots of beats 3 and 4. A Ca_i sinkhole⁸ is shown at frame 2112 ms (white arrow) at the focal discharge site (yellow arrow, frame 2312 ms).

Large diastolic Ca_i elevation and focal discharge during acetylcholine infusion

During acetylcholine infusion, six episodes in which a long pause was followed by spontaneous initiation of AF were documented in four preparations. The initiating focal discharge was captured in one episode (from the same preparation shown in Figure 1; see data supplement Movie I). Figure 2A shows the pseudo-ECG registering this episode. Panels B1 and B2 show the expanded portions of the tracing in the first and the second red rectangles, respectively, in panel A. After a long pause, two spontaneous consecutive focal discharges (red arrows, B1) originated from the LSPV, initiating consecutive LSPV–LA reentry (at cycle length of 60 ms) and atrial tachycardia for 9 seconds before spontaneous degeneration into AF (red arrow, B2). Panel C shows simultaneous Ca_i and V_m tracings of the period labeled by the red bar in panel B1. Panel D shows a further expanded portion of panel C (red bar). As expected after a long pause, the first spontaneous focal discharge was followed by a large Ca_i transient. Due to acetylcholine infusion, the APD associated with the first beat was abbreviated, resulting in diastolic elevation of Ca_i and a second discharge (red arrow, D), compatible with late phase 3 early afterdepolarizations-induced triggered activity. Isochronal maps of these two beats (E2 and E3) show the earliest activation site at the proximal LSPV, the same as that in Figure 1D.

PV focal discharge could be induced by S_1S_2 pacing protocols (2/9 at baseline; 6/9 with acetylcholine) and burst atrial pacing (7/9 at baseline; 9/9 with acetylcholine). Large Ca_i elevation is also associated with focal discharge induced by burst pacing protocols. Figure 3 shows an example of burst LA pacing-induced consecutive focal discharges from the left inferior PV (LIPV) with acetylcholine. Panel A shows the mapped field. Panels B and C show representative isochronal maps during LA pacing and LIPV focal discharge, respectively. Panel D shows the simultaneous Ca_i (yellow) and V_m (white) tracings at LIPV focal discharge site (asterisk, A). Due to shortened APD, we were able to pace LA at rapid rates. At cessation of the pacing period (green bar) was a pause during which Ca_i had time to decline. Subsequent activation was followed by a large Ca_i elevation (white arrow). The abbreviation of APD by acetylcholine resulted in Ca_i elevation during late phase 3 (red arrow), followed by a focal discharge. Subsequent activations showed consecutive focal discharges (asterisks, D) originated from the same site at the mean cycle length of 104 ± 22 ms ($N = 12$ beats), then stopped. This sequence of event was similar to that reported by Burashnikov and Antzelevitch³ in canine right atria.

Focal source AF during acetylcholine infusion

Sustained (>30 s) AF could be induced in 5 of 9 preparations at baseline and in 8 of 9 preparations with acetylcholine infusion. Before acetylcholine, baseline AF was characterized by reentrant wavefronts in the LA with intermittent conduction into the PV and occasional PV focal discharges. However, with acetylcholine the activation patterns showed PV focal discharges that competed with reentry in the LA.

Figure 4 shows an example of mixed focal discharge and reentry during acetylcholine infusion. Panel A is the pseudo-ECG showing repetitive activations and initiation of AF during baseline

(S₁) pacing. Panel B shows V_m tracings at the LA and PV focal discharge site (labeled a and b, respectively, in panel C) corresponding to this episode. Red asterisks indicate consecutive focal discharges during the initiation of AF. Panel C shows the mapped field. The isochronal maps in panel D correspond to the labeled period in panel B (red bar). Time zero for each isochronal map started at the timing below each map. After three cycles of PV–LA reentry (white circles, 204 ms, 276 ms, and 344 ms), the first PV focal discharge (black arrow, 416 ms) concurred with the fourth PV–LA reentry (white circle, 416 ms) and the second PV focal discharge (black arrow, 472 ms) occurred earlier than the fifth PV–LA reentry (white circle, 484 ms). The consecutive focal discharges lasted for 19 beats at a mean cycle length of 60 ± 3 ms, shorter than that of the coexisting PV–LA reentrant wavefronts (68 ± 9 ms, $N = 19$; $P = .0007$) in this episode. Panel E is the dominant frequency map of AF, showing the site (white arrow) of the highest dominant frequency (20.8 Hz) colocalized with the PV focal discharge site. The coexistence of consecutive PV focal discharges and PV–LA reentrant wavefronts was found in 6 of 9 preparations.

Figure 5 further illustrates the correlation between dominant frequency of AF and focal discharge. Panel A shows the mapped region. Panel B shows a typical example illustrating the isochronal map of focal discharge. Panels C and D are the dominant frequency maps of AF before and during acetylcholine infusion in the same preparation, respectively. Baseline AF showed the dominant frequency of LA was higher than that of PVs. It was due to functional conduction block between LA and PVs and a lower overall incidence of PV focal discharge during baseline AF (2.4 ± 0.6 beats/s, $N = 4$ preparations). During acetylcholine infusion, the spatial distribution of dominant frequency was changed to a focal source pattern, with the highest dominant frequency site (yellow arrow, D) colocalized with the focal discharge site at proximal LSPV (black arrow, B). The overall incidence of PV focal discharge during cholinergic AF was 6.5 ± 2.2 beats/s ($N = 8$ preparations), higher than that of baseline AF ($P = .003$). The focal source pattern was shown in 35 of 37 cholinergic AF episodes in eight preparations.

The mean cycle lengths of consecutive focal discharges and PV–LA reentrant wavefronts were shortened by acetylcholine from 161 ± 41 ms ($N = 8$) to 83 ± 44 ms ($N = 8$; $P < .001$) and from 190 ± 85 ms ($N = 4$) to 90 ± 40 ms ($N = 6$), respectively. In five preparations with inducible sustained (>30 s) AF, the mean maximum dominant frequency of AF was increased by acetylcholine from 8.7 ± 0.7 Hz to 23.6 ± 7.6 Hz ($P = .009$).

Effects of ryanodine and thapsigargin on PV arrhythmogenesis

In this study, ryanodine and thapsigargin were used to test the hypothesis that inhibition of sarcoplasmic reticulum function suppresses the inducibility of PV focal discharge and AF in six preparations. Figures 6A and 6B show an example from the same dog represented in Figure 5. Burst atrial pacing induced AF that lasted for 30 seconds (Aa). Acetylcholine prolonged the AF duration to >12 minutes. Defibrillation shocks (red arrows, Ab) were needed to terminate AF. After thapsigargin and ryanodine, only short runs of atrial tachycardia could be induced (Ac). Figure 6Ba shows the induction of 12-beat atrial arrhythmia by S₁S₂ pacing protocols. Red arrows indicate focal discharge beats from the LSPV, as shown in Figure 5B. During acetylcholine infusion, AF was induced and lasted for >12 minutes (Bb). After thapsigargin and ryanodine, only two beats were induced in this preparation (Bc). Thapsigargin and ryanodine suppressed PV focal discharge in all six preparations and AF inducibility in four of six preparations. Sustained AF (>30 s) was still inducible with thapsigargin and ryanodine in two preparations. Intermittent PV–LA reentrant wavefronts (Figures 6C and 6D, same dog as shown in Figure 4) but not focal discharges are present during these AF episodes.

Clustering of autonomic nerve endings at PV focal discharge sites

Histologic examination of PVs was performed in nine discharging and seven nondischarging PVs from seven preparations. At the focal discharge sites, abundant nerve structures and PAS-positive cells were present. For discharging PVs, the highest densities of ChAT-positive nerve structures were $1.31 \pm 0.99 \times 10^5 \mu\text{m}^2/\text{mm}^2$. These structures included both large ChAT-positive nerves (Figure 7, panels A and B) and ChAT-positive ganglia (inset G). For nondischarging PVs, density was $0.19 \pm 0.22 \times 10^5 \mu\text{m}^2/\text{mm}^2$ ($P = .01$). The density of TH-positive nerve structures (panels C and D) were $1.00 \pm 0.104 \times 10^5 \mu\text{m}^2/\text{mm}^2$ for discharging PVs and $0.46 \pm 0.58 \times 10^5 \mu\text{m}^2/\text{mm}^2$ for nondischarging PVs, respectively ($P = \text{NS}$). Panels E and F show typical examples of PAS-positive cells sectioned across the fiber.

Discussion

We found that isolated PVs from dogs with heart failure may develop ectopic rhythms that compete with sinus rhythm. After APD was shortened by acetylcholine, the same sites might serve as sources of rapid activations during AF. Histologic findings at these sites showed abundant PAS-positive cells and rich parasympathetic innervation. These findings imply that Ca_i dynamics are important in promoting triggered activity during acetylcholine infusion in PVs from pacing-induced heart failure.

Late phase 3 early afterdepolarizations

By simultaneous V_m and Ca_i mapping, we documented that pause-related large Ca_i elevation is associated with focal discharge in the PVs from heart failure dogs. Because APD was abbreviated by acetylcholine, this large rise of Ca_i resulted in persistent Ca_i elevation into late phase 3. Persistent Ca_i elevation in phase 3 of the action potential may activate the NCX current and induce late phase 3 early afterdepolarizations.^{3,4,9} These late phase 3 early afterdepolarizations initiate focal discharge and AF. We propose that this mechanism underlies the focal discharges observed in the present study. Failing hearts have increased NCX current,⁵ which makes them susceptible to late phase 3 early afterdepolarizations. Acetylcholine may increase Na^+ conductance and intracellular Na^+ activity, leading to altered NCX, reducing Ca_i efflux,^{10,11} and further enhancing Ca_i accumulation. A long preceding pause increases accumulation of intracellular Ca, leading to larger sarcoplasmic reticulum Ca release in the first beat after the pause.³ This latter phenomenon, in addition to APD shortening induced by acetylcholine, contributes to the development of late phase 3 Ca_i elevation. The combination of late phase 3 Ca_i elevation and the hyperactive NCX current facilitates the development of focal discharge from the PVs in heart failure. The hypothesis is also supported by the suppression of late phase 3 early afterdepolarizations by ryanodine and thapsigargin.

Ca_i dynamics and cholinergic AF in heart failure

We previously showed that sympathetic stimulation and low-dose ryanodine infusion can induce spontaneous sarcoplasmic reticulum calcium release, triggered activity, and focal discharges from PVs in normal dogs.⁶ These manipulations did not cause significant APD shortening to induce late phase 3 early afterdepolarizations. Rather, they facilitate the development of delayed afterdepolarizations. However, in the present study, we showed that APD abbreviation associated with diastolic Ca_i elevation by acetylcholine can precipitate PV focal discharge in a heart failure canine model. As the inherent paucity of I_{K1} in PV myocytes,¹² abnormal Ca_i handling is apt to cause membrane depolarization in these cells. Heart failure is associated with increased sympathetic and vagal discharges.¹ Parasympathetic activation and acetylcholine release could be important mechanisms in the pathophysiology and atrial arrhythmogenesis of heart failure status. Livanis et al¹³ reported that neurally mediated mechanisms may be implicated in the pathophysiology of syncope in patients with dilated

cardiomyopathy. In that study, both sympathetic and parasympathetic heart rate parameters were markedly stimulated.

Focal discharge and reentry in focal source AF

Kalife et al¹⁴ reported that increasing intra-LA pressure facilitates stable rotors at the PV–LA junction to drive AF. With acetylcholine administration in canine PV preparations, Po et al¹⁵ showed that sustained reentry underlies the mechanisms of induced PV tachycardia. However, Patterson et al⁹ showed that early afterdepolarizations formation and triggered arrhythmias were initiated by combined parasympathetic and sympathetic nerve stimulation. In the present study, we demonstrated the coexistence of PV focal discharge and PV–LA microreentry during cholinergic AF. For example, Figure 2 documented that sustained arrhythmias can be induced by two beats of triggered activity followed by sustained reentry. However, Figure 3 shows sustained focal discharges. The mechanism of these sustained focal discharges likely is L-type calcium current (I_{Ca-L}) facilitation during repetitive high-rate activations.¹⁶ The increased I_{Ca-L} helps to increase Ca_i and the NCX current, sustaining the triggered activity. The mechanisms of frequency-dependent facilitation of I_{Ca-L} were thought to reflect reduced Ca-dependent inactivation related to reduced Ca load and sarcoplasmic reticulum Ca release.¹⁷ Thapsigargin, which inhibits sarcoplasmic reticulum Ca release, eliminates I_{Ca-L} facilitation during the high rate of activation.¹⁷ These latter findings are consistent with our results showing that thapsigargin and ryanodine prevented induction of triggered activities. We also found that the cycle lengths of focal discharge were shorter than reentry and the sites of highest dominant frequency during cholinergic AF were highly colocalized with the sites of PV focal discharge. These findings suggest that both triggered and reentrant activities are important during cholinergic focal source AF.

Study limitations

Whether or not PAS-positive cells contribute to the onset of focal discharge is unknown. Allesie et al¹⁸ estimated that a minimum area of 30 to 50 mm² is required to accommodate circus movement reentry in rabbit atria. The thickness of canine PV muscle sleeves at the site of focal discharges is insufficient to support transmural reentry of that size. However, we do not have methods for detailed transmural mapping of PV muscle sleeves to completely rule out transmural reentry at the focal discharge site.

Supplementary Material

Refer to Web version on PubMed Central for supplementary material.

Acknowledgments

This study was supported by CMRPG33016 to Dr. Chou, a Piansky Endowment to Dr. Fishbein, a Pauline and Harold Price Endowment and Medtronic-Zipes Endowment to Dr. Chen. This study was supported in part by an AHA Established Investigatorship Award and by NIH Grants P01-HL78931, R01-HL58533, 66389, 78932, and 71140.

We thank Avile McCullen, Lei Lin, and Elaine Lebowitz for assistance.

References

1. Ogawa M, Zhou S, Tan AY, et al. Left stellate ganglion and vagal nerve activity and cardiac arrhythmias in ambulatory dogs with pacing-induced congestive heart failure. *J Am Coll Cardiol* 2007;50:335–343. [PubMed: 17659201]
2. Kneller J, Zou R, Vigmond EJ, et al. Cholinergic atrial fibrillation in a computer model of a two-dimensional sheet of canine atrial cells with realistic ionic properties. *Circ Res* 2002;90:E73–E87. [PubMed: 12016272]

3. Burashnikov A, Antzelevitch C. Reinduction of atrial fibrillation immediately after termination of the arrhythmia is mediated by late phase 3 early afterdepolarization-induced triggered activity. *Circulation* 2003;107:2355–2360. [PubMed: 12695296]
4. Patterson E, Lazzara R, Szabo B, et al. Sodium-calcium exchange initiated by the Ca^{2+} transient: an arrhythmia trigger within pulmonary veins. *J Am Coll Cardiol* 2006;47:1196–1206. [PubMed: 16545652]
5. Li D, Melnyk P, Feng J, et al. Effects of experimental heart failure on atrial cellular and ionic electrophysiology. *Circulation* 2000;101:2631–2638. [PubMed: 10840016]
6. Chou C-C, Nihei M, Zhou S, et al. Intracellular calcium dynamics and anisotropic reentry in isolated canine pulmonary veins and left atrium. *Circulation* 2005;111:2889–2297. [PubMed: 15927973]
7. Cao J-M, Fishbein MC, Han JB, et al. Relationship between regional cardiac hyperinnervation and ventricular arrhythmia. *Circulation* 2000;101:1960–1969. [PubMed: 10779463]
8. Hwang G-S, Hayashi H, Tang L, et al. Intracellular calcium and vulnerability to fibrillation and defibrillation in Langendorff-perfused rabbit ventricles. *Circulation* 2006;114:2595–2603. [PubMed: 17116770]
9. Patterson E, Po SS, Scherlag BJ, et al. Triggered firing in pulmonary veins initiated by in vitro autonomic nerve stimulation. *Heart Rhythm* 2005;2:624–631. [PubMed: 15922271]
10. Tajima T, Tsuji Y, Sorota S, et al. Positive vs. negative inotropic effects of carbachol in avian atrial muscle: role of Ni-like protein. *Circ Res* 1987;61:I105–I111. [PubMed: 3115621]
11. Matsumoto K, Pappano AJ. Sodium-dependent membrane current induced by carbachol in single guinea-pig ventricular myocytes. *J Physiol* 1989;415:487–502. [PubMed: 2561791]
12. Ehrlich JR, Cha TJ, Zhang L, et al. Cellular electrophysiology of canine pulmonary vein cardiomyocytes: action potential and ionic current properties. *J Physiol* 2003;551:801–813. [PubMed: 12847206]
13. Livanis EG, Kostopoulou A, Theodorakis GN, et al. Neurocardiogenic mechanisms of unexplained syncope in idiopathic dilated cardiomyopathy. *Am J Cardiol* 2007;99:558–562. [PubMed: 17293203]
14. Kalifa J, Jalife J, Zaitsev AV, et al. Intra-atrial pressure increases rate and organization of waves emanating from the superior pulmonary veins during atrial fibrillation. *Circulation* 2003;108:668–671. [PubMed: 12900337]
15. Po SS, Li Y, Tang D, et al. Rapid and stable re-entry within the pulmonary vein as a mechanism initiating paroxysmal atrial fibrillation. *J Am Coll Cardiol* 2005;45:1871–1877. [PubMed: 15936621]
16. Piot C, Lemaire S, Albat B, et al. High frequency-induced upregulation of human cardiac calcium currents. *Circulation* 1996;93:120–128. [PubMed: 8616918]
17. Delgado C, Artilés A, Gomez AM, et al. Frequency-dependent increase in cardiac Ca^{2+} current is due to reduced Ca^{2+} release by the sarcoplasmic reticulum. *J Mol Cell Cardiol* 1999;31:1783–1793. [PubMed: 10525417]
18. Allesie MA, Bonke FI, Schopman FJ. Circus movement in rabbit atrial muscle as a mechanism of tachycardia. III. The “leading circle” concept: a new model of circus movement in cardiac tissue without the involvement of an anatomical obstacle. *Circ Res* 1977;41:9–18. [PubMed: 862147]

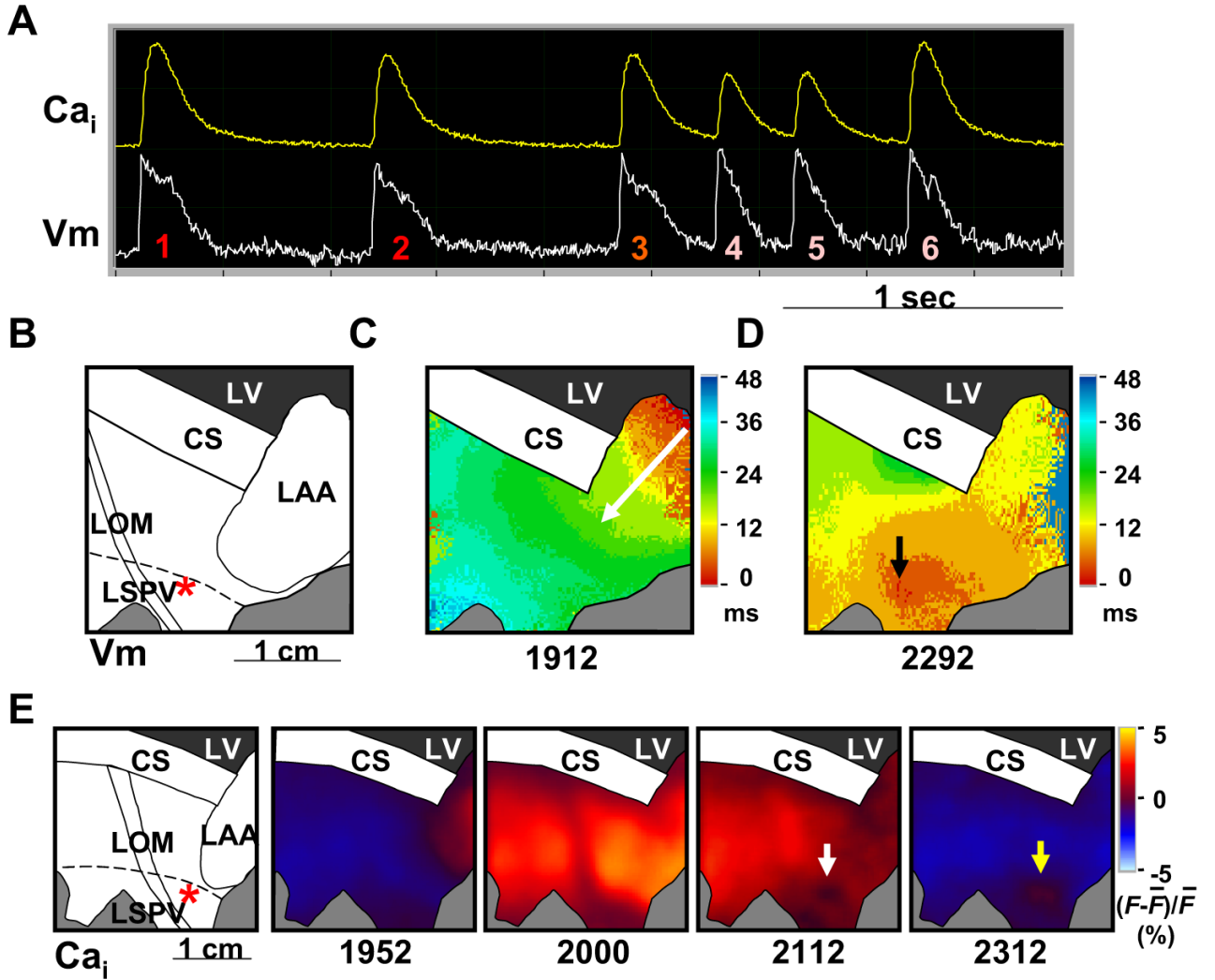


Figure 1.

Spontaneous atrial activities in isolated pulmonary vein–left atrial preparation at baseline.

A: Intracellular calcium (Ca_i ; yellow) and membrane potential (V_m ; white) optical recordings at site of focal discharge (*asterisk* in B). **B:** Mapped field. **C:** Representative isochronal map of beats 1–3 showing activation wavefront invaded the mapped region from the right edge (*white arrow*). **D:** Representative isochronal map of beats 4–6 showing earliest activation at the left superior pulmonary vein (*black arrow*). **E:** Ratio maps of Ca_i showing Ca_i sinkhole (*white arrow*) at the site of pulmonary vein focal discharge (*yellow arrow*). The number below each subpanel is the time, with the beginning of data acquisition as time zero. CS = coronary sinus; LAA = left atrial appendage; LOM = ligament of Marshall; LSPV = left superior pulmonary vein; LV = left ventricle.

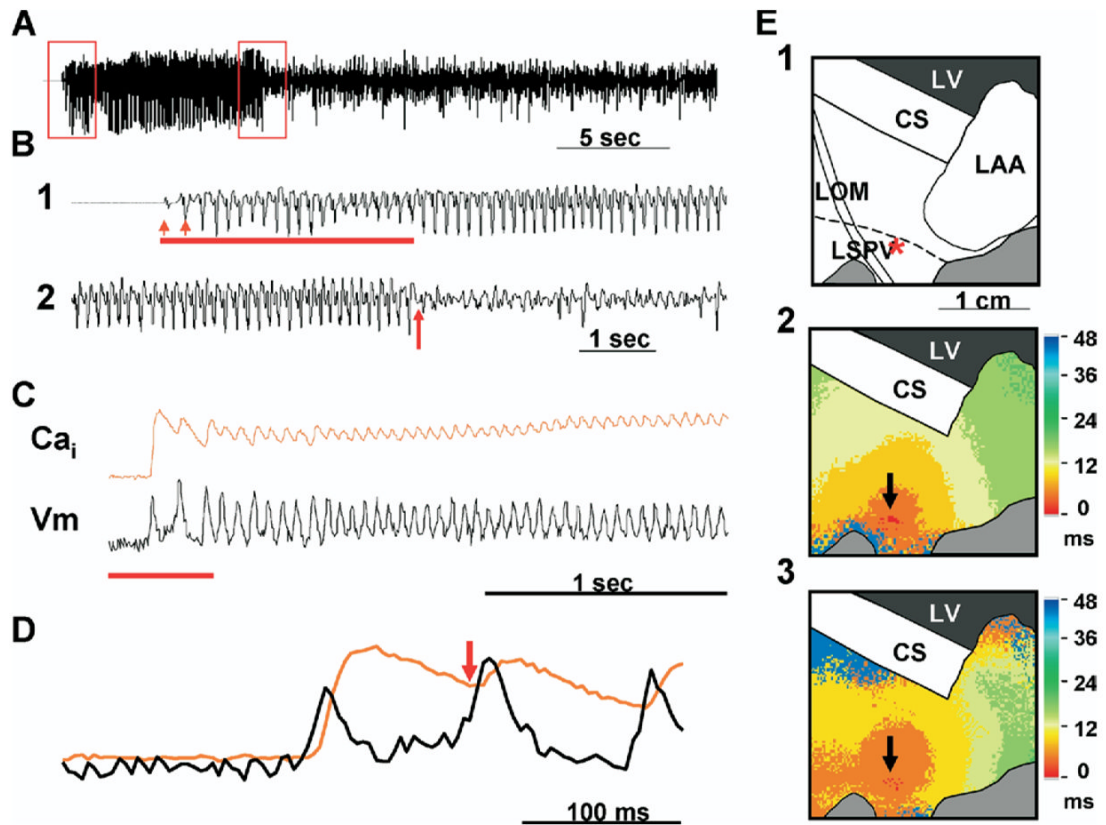


Figure 2. Spontaneous atrial fibrillation initiation by pulmonary vein (PV) focal discharges with acetylcholine. **A, B:** Pseudo-ECG and the expanded portions, respectively. *Arrows* indicate PV initiators (B1) and transition from atrial tachycardia to AF (**B2**). **C, D:** Intracellular calcium (Ca_i ; orange) and membrane potential (V_m ; black) optical recordings and amplified signals, respectively. *Red arrow* indicates elevated diastolic Ca_i level. **E1, E2, E3:** Isochronal maps of the first and second left superior pulmonary vein (LSPV) focal discharges, respectively. CS = coronary sinus; LAA = left atrial appendage; LOM = ligament of Marshall; LV = left ventricle.

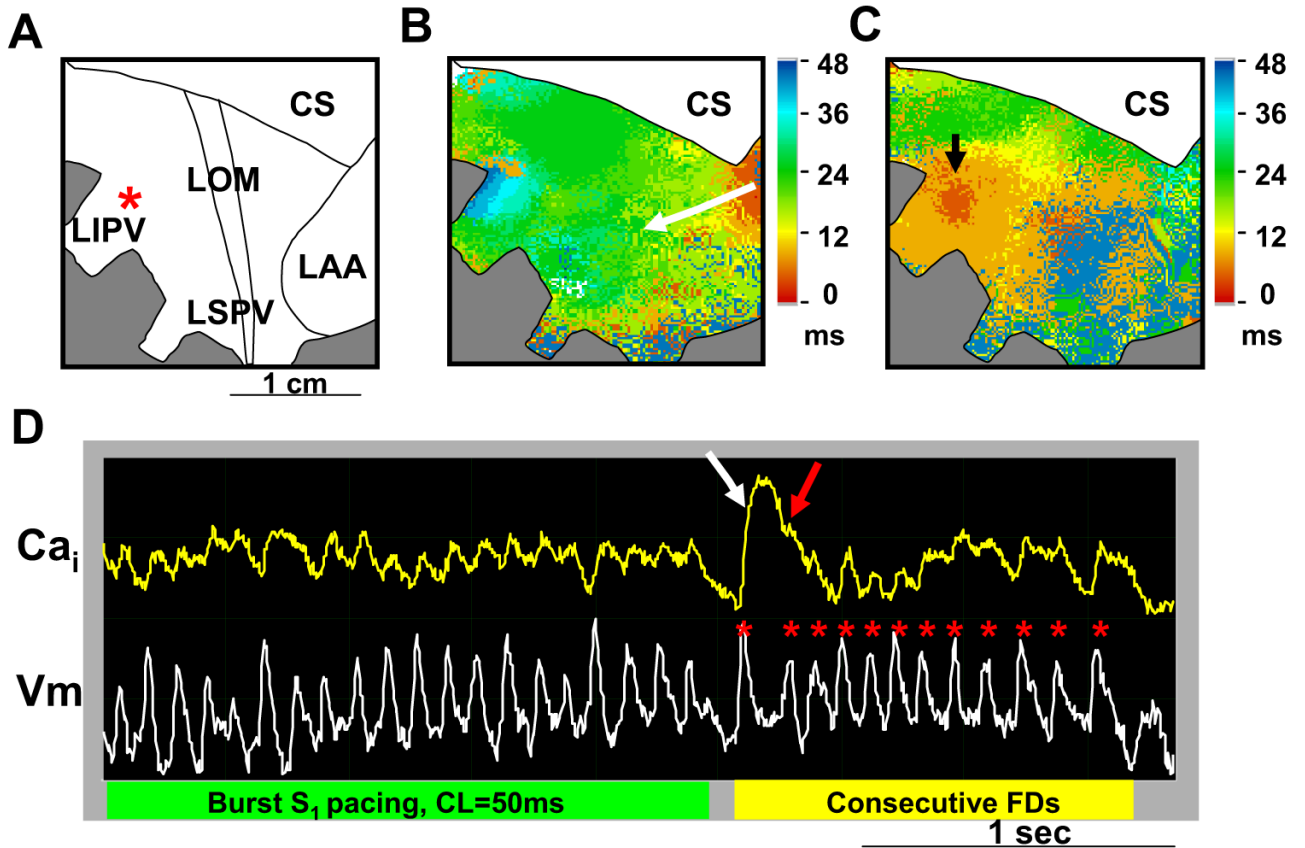


Figure 3. Burst left atrial (LA)-pacing induced consecutive pulmonary vein (PV) focal discharges with acetylcholine. **A:** Mapped field. **B, C:** Isochronal maps of representative LA pacing beat and left inferior pulmonary vein (LIPV) focal discharge, respectively. *White arrow* indicates wavefront propagating from right border of the mapped field to PVs during LA pacing. *Black arrow* indicates LIPV focal discharge. **D:** Intracellular calcium (Ca_i ; yellow) and membrane potential (V_m ; white) optical recordings at site of focal discharge (*asterisk* in **A**). *White arrow* indicates large Ca_i transient accompanying the first focal discharge. *Red arrow* indicates elevated diastolic Ca_i level. *Red asterisks* indicate consecutive focal discharges. CS = coronary sinus; LAA = left atrial appendage; LOM = ligament of Marshall; LSPV = left superior pulmonary vein.

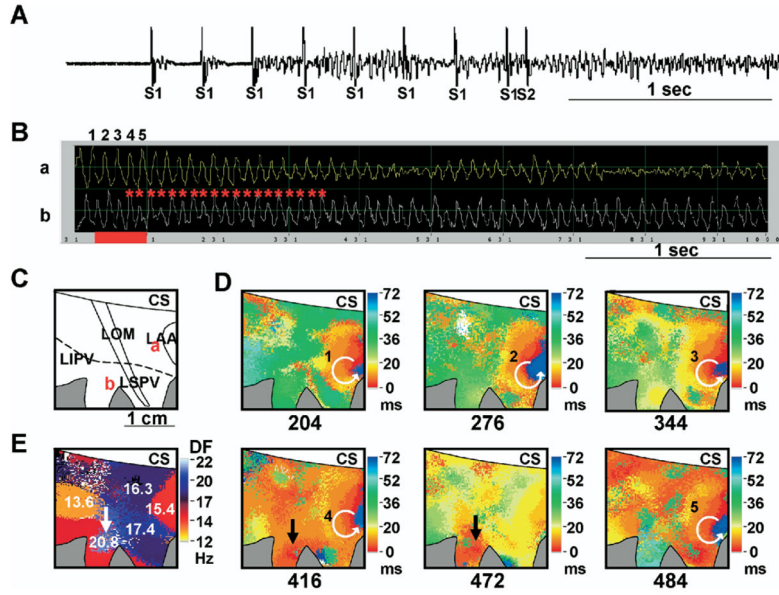


Figure 4. Spontaneous atrial fibrillation initiation during S_1 pacing with acetylcholine. **A:** Pseudo-ECG. **B:** Optical membrane potential (V_m) recordings at left atrial (site a) and left superior pulmonary vein (PV) focal discharge site (site b) labeled in C. *Red asterisks* indicate consecutive focal discharges. **C:** Mapped field. **D:** Isochronal maps showing consecutive microreentrant wavefronts (*white circles*) and PV focal discharges (*black arrows*) corresponding to V_m tracings labeled by the numbers 1–5 and the first two asterisks in B, respectively. **E:** Dominant frequency map of this atrial fibrillation episode. *White arrow* indicates highest dominant frequency (DF). CS = coronary sinus; LAA = left atrial appendage; LIPV = left inferior pulmonary vein; LOM = ligament of Marshall; LSPV = left superior pulmonary vein.

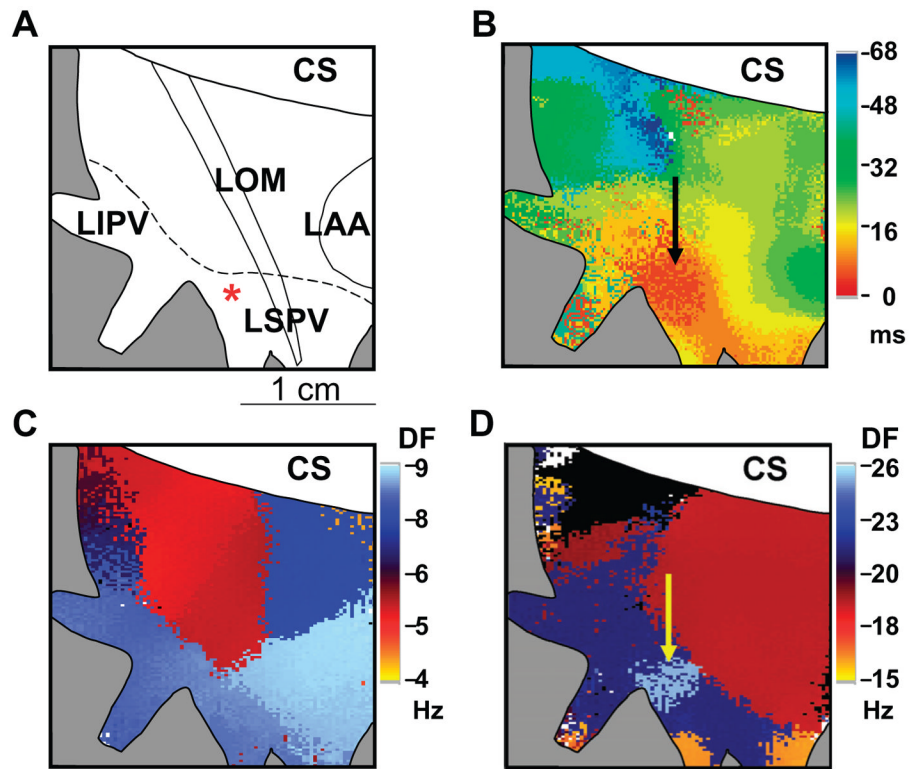


Figure 5. Focal source atrial fibrillation with acetylcholine. **A:** Mapped field. **B:** Isochronal map of pulmonary vein focal discharge. **C, D:** Dominant frequency maps at baseline and cholinergic atrial fibrillation, respectively. CS = coronary sinus; LAA = left atrial appendage; LIPV = left inferior pulmonary vein; LOM = ligament of Marshall; LSPV = left superior pulmonary vein.

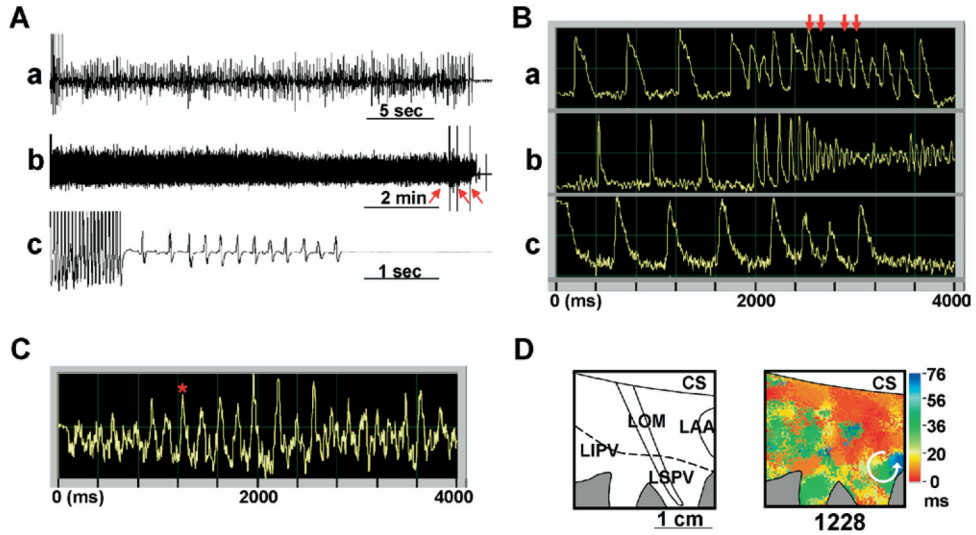


Figure 6. Effects of acetylcholine, ryanodine, and thapsigargin on atrial arrhythmias. **A:** Pseudo-ECG showing burst atrial pacing-induced arrhythmias at baseline (a), with acetylcholine (b), and after ryanodine and thapsigargin (c). *Red arrows* indicate spikes due to electrical shocks. **B:** Optical membrane potential (Vm) recordings showing S_1S_2 pacing-induced arrhythmias at baseline (a), with acetylcholine (b), and after ryanodine and thapsigargin (c). *Reds arrows* indicate pulmonary vein focal discharges. **C:** Optical Vm recording of AF with ryanodine and thapsigargin. **D: left,** mapped field; **right,** isochronal map of pulmonary vein-left atrial reentry during AF in C (*asterisk*). CS = coronary sinus; LAA = left atrial appendage; LIPV = left inferior pulmonary vein; LOM = ligament of Marshall; LSPV = left superior pulmonary vein.

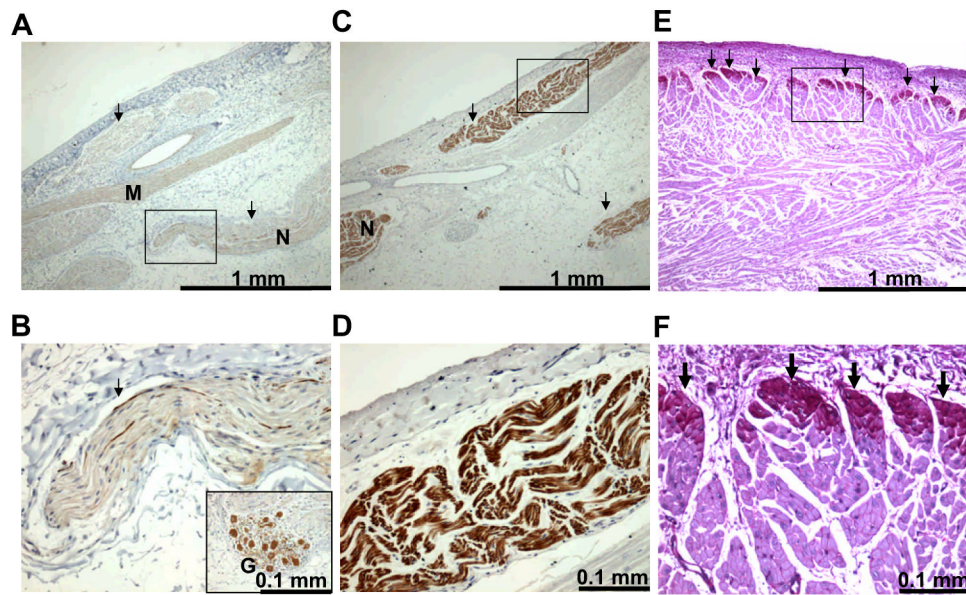


Figure 7. Autonomic nerve and periodic acid–Schiff (PAS) staining at the focal discharge site. *Arrows* indicate structures stained positive for anti-choline acetyl-transferase (**A**), anti-tyrosine hydroxylase (**C**), and PAS (**E**). **B, D, F:** Magnified view of the rectangular areas in **A, C,** and **E,** respectively. Subendocardial PAS-positive cells (*black arrows*) were sectioned horizontally. Inset **G** shows a parasympathetic ganglion from the same slide shown in **A**. M = myocardium; N = nerve bundle.